On timelike and spacelike deeply virtual Compton scattering at next to leading order

Jakub Wagner

Theoretical Physics Department
National Center for Nuclear Research, Warsaw

DIS2013, April 24th

in collaboration with B. Pire (CPhT Ecole Polytechnique, Palaiseau) L. Szymanowski (NCNR, Warsaw) H. Moutarde and F. Sabatié (CEA, Saclay) - Phys. Rev. D87 (2013) 054029

Outline

DVCS

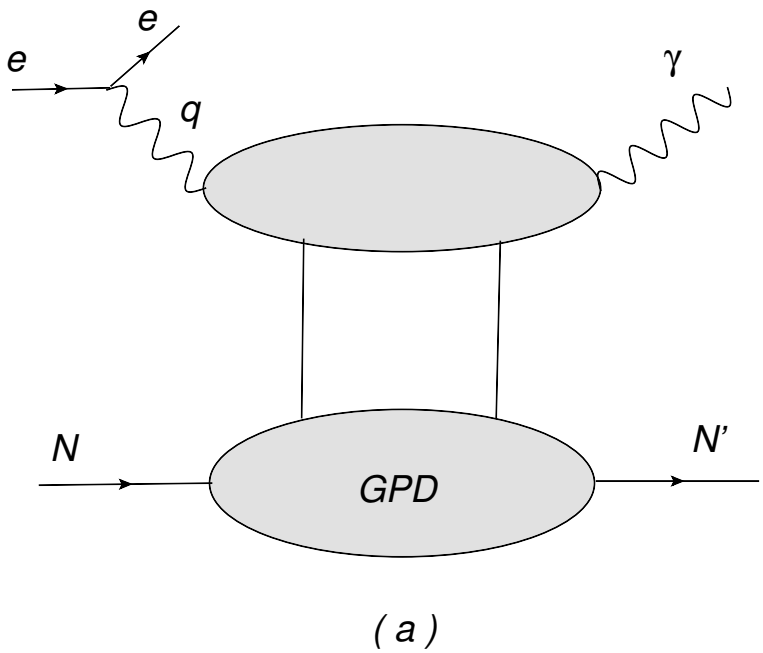

Figure: Deeply Virtual Compton Scattering : $lN \to l'N'\gamma$

TCS

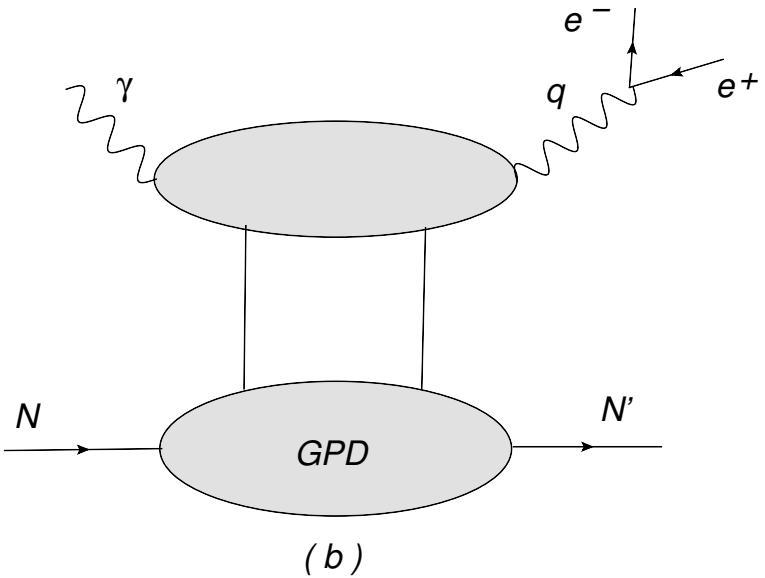

Figure: Timelike Compton Scattering: $\gamma N \to l^+ l^- N'$

DVCS is the golden channel, so why TCS?

- GDPs enter factorization theorems for hard exlusive reactions (DVCS, deeply virtual meson production, TCS etc.), in a similar manner as PDFs enter factorization theorem for DIS
- First moment of GPDs enters the Ji's sum rule for the angular momentum carried by partons in the nucleon,
- Deeply Virtual Compton Scattering (DVCS) is a golden channel for GPDs extraction,
- Why TCS: universality of the GPDs, another source for GPDs (special sensitivity on real part), spacelike-timelike crossing and understanding the structure of the NLO corrections,
- Experiments: CLAS 6 GeV $\rightarrow$ CLAS 12 GeV, COMPASS, RHIC, LHC ?

Motivation for NLO

Why do we need NLO corrections:

- gluons enter at NLO,
- DIS versus Drell-Yan: big K-factors $\log \frac{-Q^2}{\mu_F^2} \to \log \frac{Q^2}{\mu_F^2} \pm i\pi,$
- reliability of the results, factorization scale dependence,

Belitsky, Mueller, Niedermeier, Schafer, Phys.Lett.B474 ,2000.
Pire, Szymanowski, Wagner, Phys.Rev.D83, 2011.

General Compton Scattering:

$$\gamma^*(q_{in})N \to \gamma^*(q_{out})N'$$

- DDVCS: $q_{in}^2 < 0\,, \quad q_{out}^2 > 0\,, \quad \eta \neq \xi$
- DVCS: $q_{in}^2 < 0\,, \quad q_{out}^2 = 0\,, \quad \eta = \xi > 0$
- TCS: $q_{in}^2 = 0\,, \quad q_{out}^2 > 0\,, \quad \eta = -\xi > 0$

Coefficient functions and Compton Form Factors

Results for spacelike and timelike Compton Form Factors (CFF) at NLO, $\mathcal{H}$ and $\widetilde{\mathcal{H}}$, defined in the DVCS case as:

$$\begin{aligned}
\mathcal{H}(\xi,t) &= +\int_{-1}^{1} dx \left(\sum_q T^q(x,\xi) H^q(x,\xi,t) + T^g(x,\xi) H^g(x,\xi,t) \right) \\
\widetilde{\mathcal{H}}(\xi,t) &= -\int_{-1}^{1} dx \left(\sum_q \widetilde{T}^q(x,\xi) \widetilde{H}^q(x,\xi,t) + \widetilde{T}^g(x,\xi) \widetilde{H}^g(x,\xi,t) \right).
\end{aligned}$$

These CFFs are the GPD dependent quantities which enter the amplitudes. For DVCS they are defined through relations:

$$\begin{aligned}
\mathcal{A}^{\mu\nu}(\xi,t) = -e^2 \frac{1}{(P+P')^+} \bar{u}(P') \Bigg[g_T^{\mu\nu} \left(\mathcal{H}(\xi,t)\,\gamma^+ + \mathcal{E}(\xi,t)\,\frac{i\sigma^{+\rho}\Delta_\rho}{2M} \right) \\
+ i\epsilon_T^{\mu\nu} \left(\widetilde{\mathcal{H}}(\xi,t)\,\gamma^+\gamma_5 + \widetilde{\mathcal{E}}(\xi,t)\,\frac{\Delta^+\gamma_5}{2M} \right) \Bigg] u(P)\,,
\end{aligned}$$

where we use $\mathcal{H}(\xi,t) = \mathcal{H}(\xi,\eta=\xi,t)$. Similar relation holds for TCS with ξ replaced by η.

Coefficient functions

Renormalized coefficient functions are given by

$$
\begin{aligned}
T^q(x) &= \left[C_0^q(x) + C_1^q(x) + \ln\left(\frac{Q^2}{\mu_F^2}\right) \cdot C_{coll}^q(x)\right] - (x \to -x)\,, \\
T^g(x) &= \left[C_1^g(x) + \ln\left(\frac{Q^2}{\mu_F^2}\right) \cdot C_{coll}^g(x)\right] + (x \to -x)\,, \\
\widetilde{T}^q(x) &= \left[\widetilde{C}_0^q(x) + \widetilde{C}_1^q(x) + \ln\left(\frac{Q^2}{\mu_F^2}\right) \cdot \widetilde{C}_{coll}^q(x)\right] + (x \to -x)\,, \\
\widetilde{T}^g(x) &= \left[\widetilde{C}_1^g(x) + \ln\left(\frac{Q^2}{\mu_F^2}\right) \cdot \widetilde{C}_{coll}^g(x)\right] - (x \to -x)\,.
\end{aligned}
$$

Results of the NLO calculations of the quark coefficient functions read in the DVCS case:

$$
\begin{aligned}
C_0^q(x,\xi) &= -e_q^2 \frac{1}{x+\xi-i\varepsilon}\,, \\
C_1^q(x,\xi) &= \frac{e_q^2\alpha_S C_F}{4\pi}\frac{1}{x+\xi-i\varepsilon}\left[9-3\frac{x+\xi}{x-\xi}\log(\frac{x+\xi}{2\xi}-i\varepsilon)-\log^2(\frac{x+\xi}{2\xi}-i\varepsilon)\right], \\
C_{coll}^q(x,\xi) &= \frac{e_q^2\alpha_S C_F}{4\pi}\frac{1}{x+\xi-i\varepsilon}\left[-3-2\log(\frac{x+\xi}{2\xi}-i\varepsilon)\right], \\
\widetilde{C}_0^q(x,\xi) &= -e_q^2 \frac{1}{x+\xi-i\varepsilon}\,, \\
\widetilde{C}_1^q(x,\xi) &= \frac{e_q^2\alpha_S C_F}{4\pi}\frac{1}{x+\xi-i\varepsilon}\left[9-\frac{x+\xi}{x-\xi}\log(\frac{x+\xi}{2\xi}-i\varepsilon)-\log^2(\frac{x+\xi}{2\xi}-i\varepsilon)\right], \\
\widetilde{C}_{coll}^q(x,\xi) &= \frac{e_q^2\alpha_S C_F}{4\pi}\frac{1}{x+\xi-i\varepsilon}\left[-3-2\log(\frac{x+\xi}{2\xi}-i\varepsilon)\right],
\end{aligned}
$$

more on $x \pm \xi$ behaviour → S.Wallon talk
T.Altinoluk, B.Pire, L.Szymanowski, S.Wallon, JHEP 1210

The results for the TCS case are simply related to these expressions:

$$
{}^{TCS}T(x,\eta) = \pm\left({}^{DVCS}T(x,\xi=\eta) + i\pi C_{coll}(x,\xi=\eta)\right)^*\,,
$$

D.Mueller, B.Pire, L.Szymanowski, J.Wagner, Phys.Rev.D86, 2012.

where $+$ $(-)$ sign corresponds to vector (axial) case.

Models

In our analysis we use two GPD models based on double distibution:

$$F_i(x,\xi,t) = \int_{-1}^{1} d\beta \int_{-1+|\beta|}^{1-|\beta|} d\alpha\, \delta(\beta+\xi\alpha-x)\, f_i(\beta,\alpha,t) + D_i^F\left(\frac{x}{\xi},t\right)\Theta(\xi^2-x^2)\,,$$

The DD f_i reads

$$f_i(\beta,\alpha,t) = g_i(\beta,t)\, h_i(\beta)\, \frac{\Gamma(2n_i+2)}{2^{2n_i+1}\Gamma^2(n_i+1)}\, \frac{[(1-|\beta|)^2-\alpha^2]^{n_i}}{(1-|\beta|)^{2n_i+1}}\,,$$

- Goloskokov-Kroll: based on CTEQ6m PDFs, $g_i(\beta,t) = \mathrm{e}^{b_i t}\,|\beta|^{-\alpha_i' t}$
- Factorized: based on MSTW08, $g_u(\beta,t) = \frac{1}{2}F_1^u(t)$

Compton Form Factors - DVCS - $Re(\mathcal{H})$

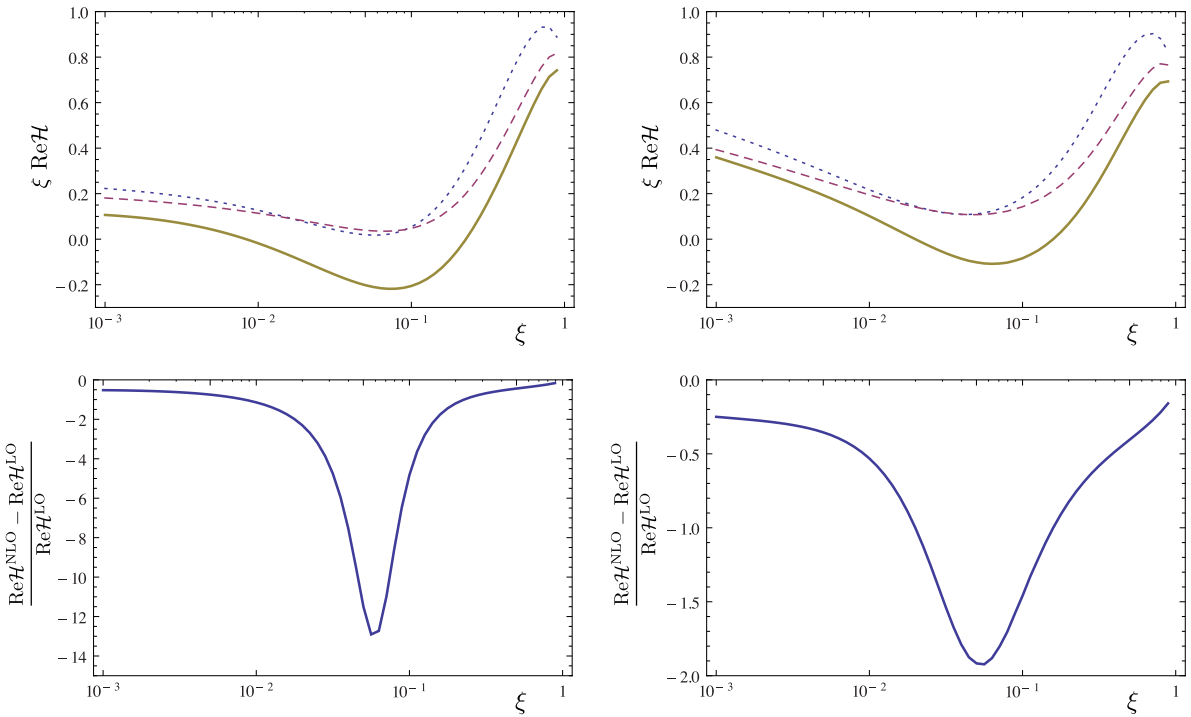

Figure: The real part of the *spacelike* Compton Form Factor $\mathcal{H}(\xi)$ multiplied by ξ, as a function of ξ in the double distribution model based on Kroll-Goloskokov (upper left) and MSTW08 (upper right) parametrizations, for $\mu_F^2 = Q^2 = 4\,\mathrm{GeV}^2$ and $t = -0.1\,\mathrm{GeV}^2$, at the Born order (dotted line), including the NLO quark corrections (dashed line) and including both quark and gluon NLO corrections (solid line). Below the ratios of the NLO correction to LO result in the corresponding models.

Compton Form Factors - DVCS - $Im(\mathcal{H})$

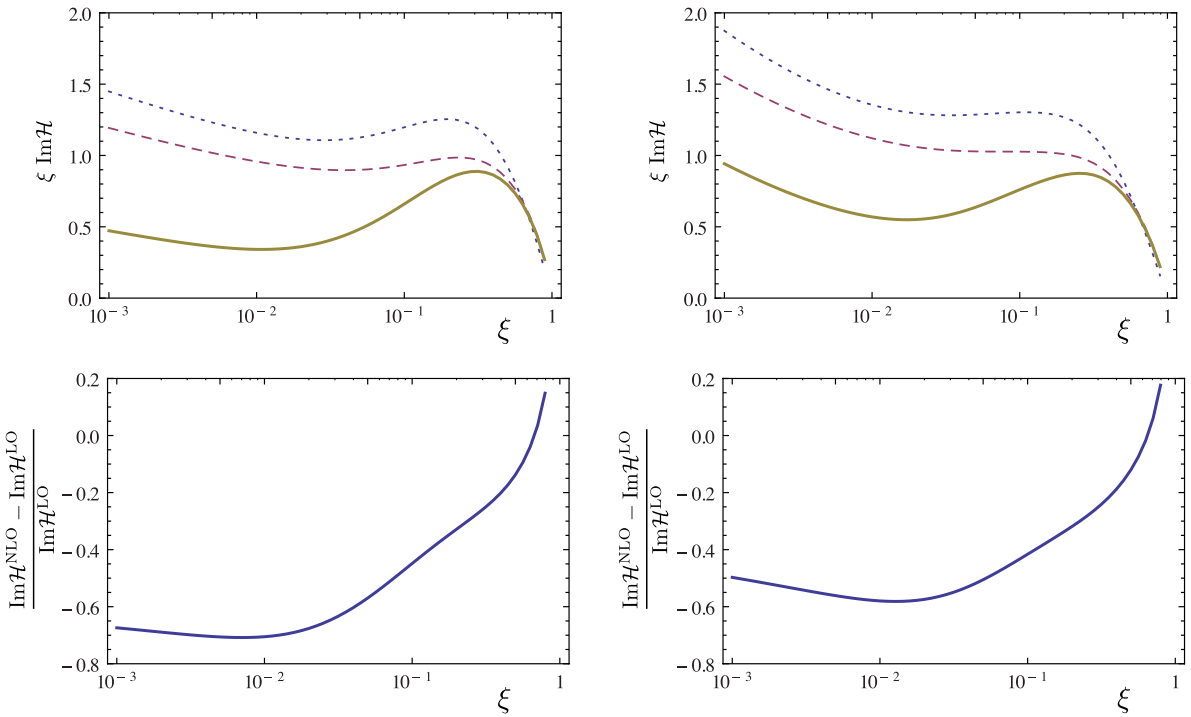

Figure: The imaginary part of the *spacelike* Compton Form Factor $\mathcal{H}(\xi)$ multiplied by ξ, as a function of ξ in the double distribution model based on Kroll-Goloskokov (upper left) and MSTW08 (upper right) parametrizations, for $\mu_F^2 = Q^2 = 4\,\mathrm{GeV}^2$ and $t = -0.1\,\mathrm{GeV}^2$, at the Born order (dotted line), including the NLO quark corrections (dashed line) and including both quark and gluon NLO corrections (solid line). Below the ratios of the NLO correction to LO result in the corresponding models.

Compton Form Factors - TCS - $Re(\mathcal{H})$

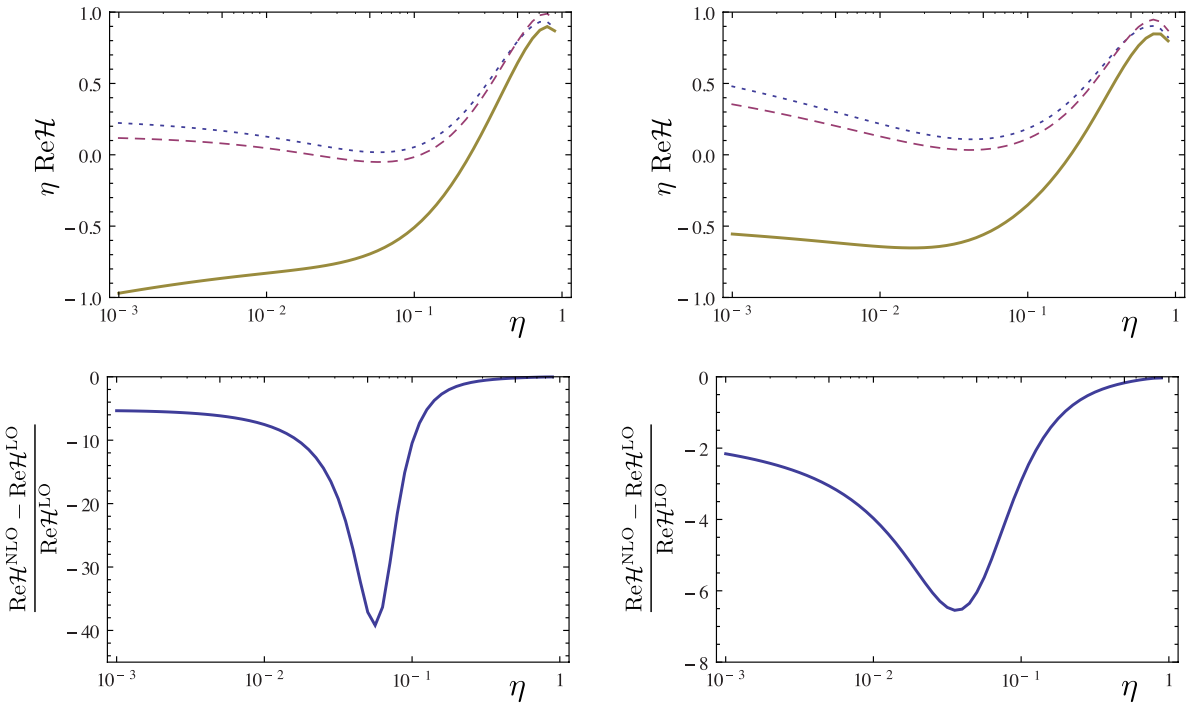

Figure: The real part of the *timelike* Compton Form Factor $\mathcal{H}$ multiplied by η, as a function of η in the double distribution model based on Kroll-Goloskokov (upper left) and MSTW08 (upper right) parametrizations, for $\mu_F^2 = Q^2 = 4$ GeV^2 and $t = -0.1$ GeV^2. Below the ratios of the NLO correction to LO result of the corresponding models.

Compton Form Factors - TCS - $Im(\mathcal{H})$

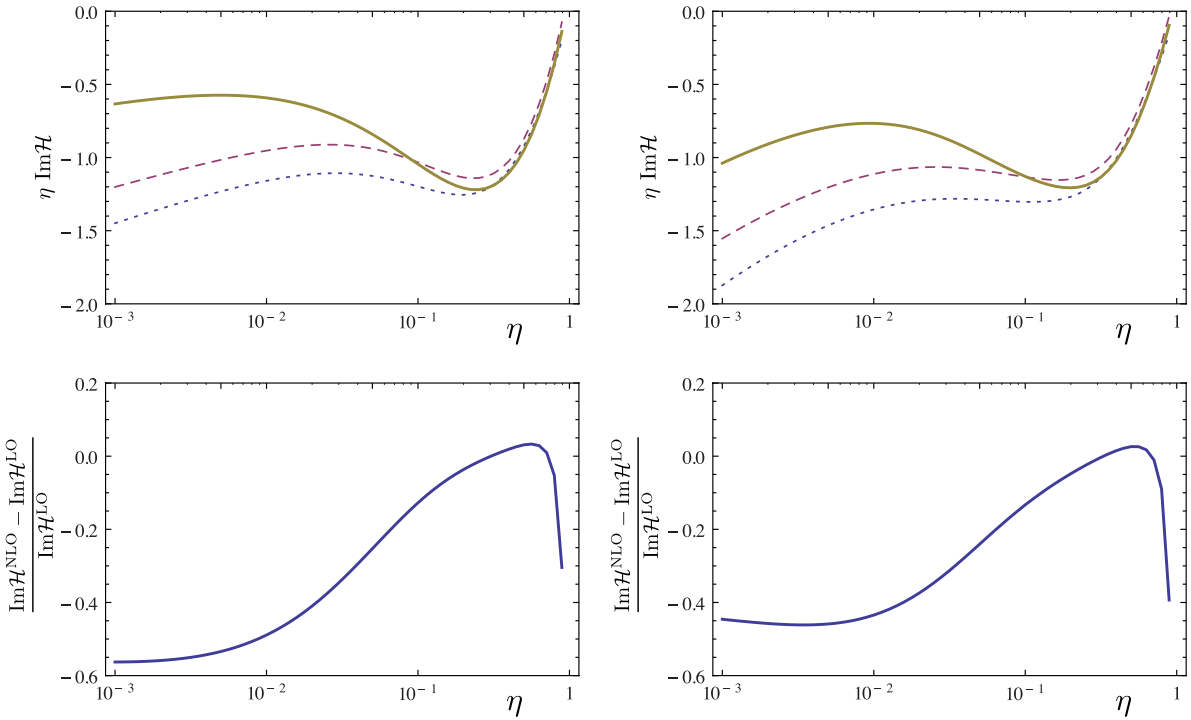

Figure: The imaginary part of the *timelike* Compton Form Factor $\mathcal{H}$ multiplied by η, as a function of η in the double distribution model based on Kroll-Goloskokov (upper left) and MSTW08 (upper right) parametrizations, for $\mu_F^2 = Q^2 = 4$ GeV^2 and $t = -0.1$ GeV^2. Below the ratios of the NLO correction to LO result of the corresponding models.

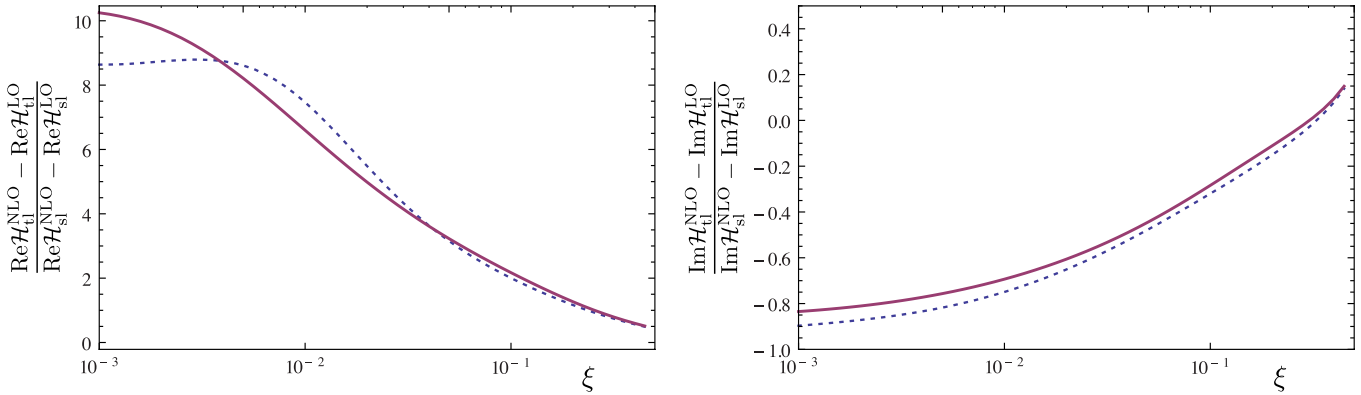

Figure: The **ratio** of the timelike to spacelike NLO corrections in the real (left) and imaginary (right) part of the CFF $\mathcal{H}$, in the GK (dashed) and factorized MSTW08 (solid)

Model (in)dependence:

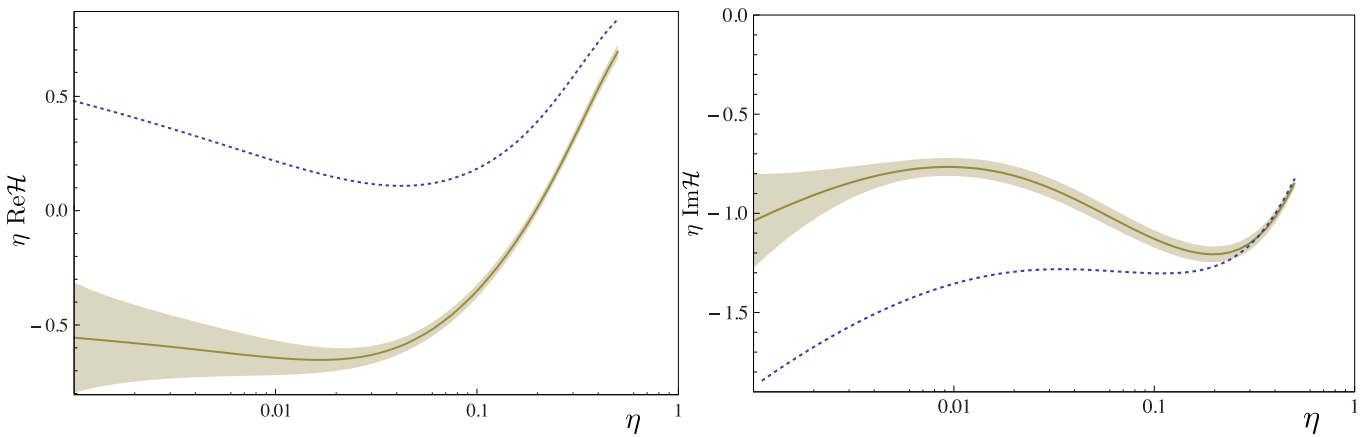

Figure: The dotted line shows the LO result and shaded bands around solid lines show the effect of a one sigma uncertainty of the input MSTW08 fit to the full NLO result.

DVCS - JLab : beam spin asymmetry

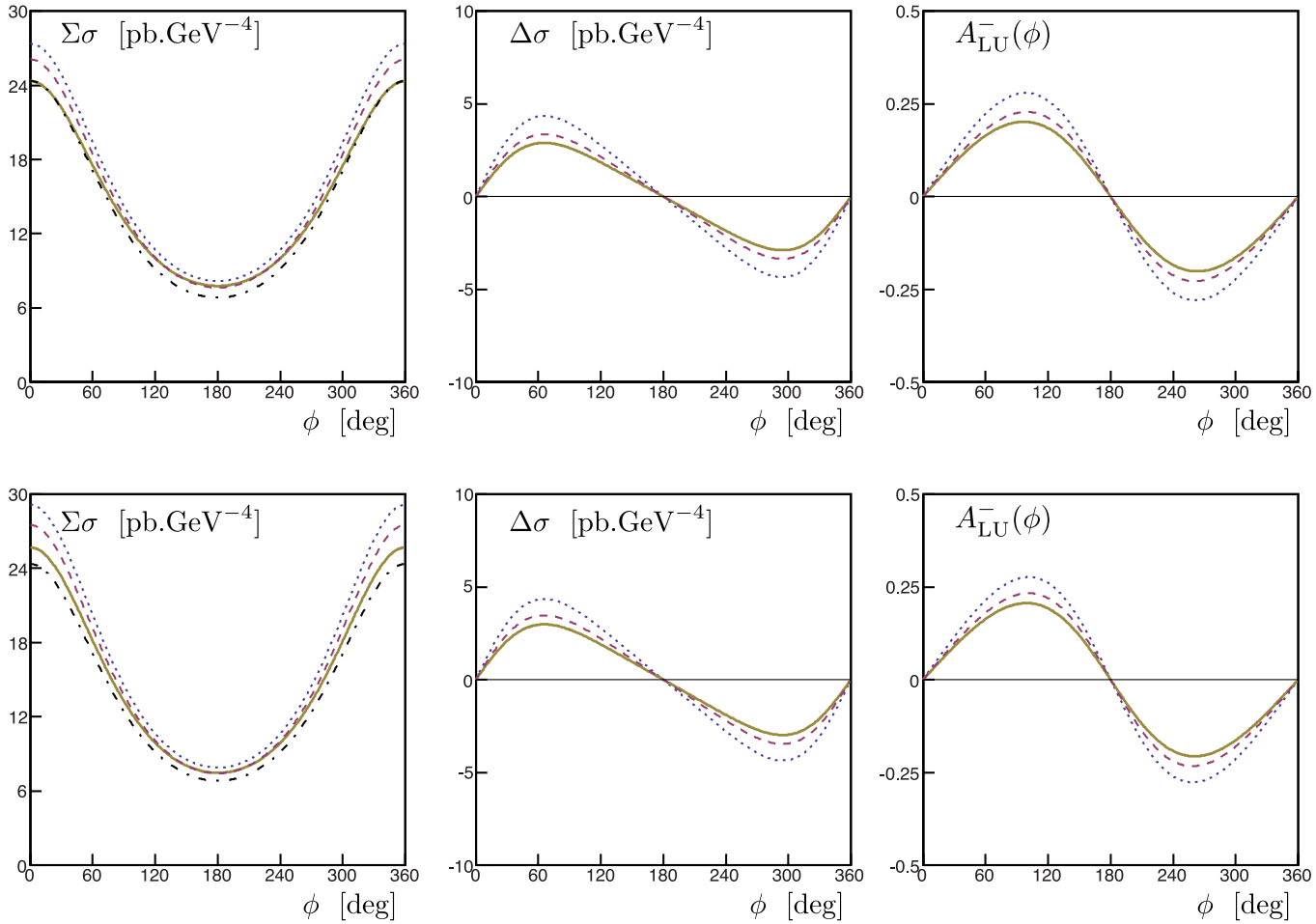

Figure: $E_e = 11\,\mathrm{GeV}, \mu_F^2 = Q^2 = 4$ GeV^2 and $t = -0.2$ GeV^2. On the first line, the GPD $H(x,\xi,t)$ is parametrized by the GK model, on the second line by factorized model based on the MSTW08 parametrization. The contributions from other GPDs are not included. In all plots, the LO - dotted line, the full NLO - solid line, NLO result without the gluonic contribution - dashed line, the BH- dashdotted line.

DVCS - COMPASS: mixed charge-spin asymmetry

$$\mathcal{S}_{\mathrm{CS,U}}(\phi) \equiv d\sigma^{\overset{+}{\rightarrow}} + d\sigma^{\overset{-}{\leftarrow}}, \mathcal{D}_{\mathrm{CS,U}}(\phi) \equiv d\sigma^{\overset{+}{\rightarrow}} - d\sigma^{\overset{-}{\leftarrow}}, \mathcal{A}_{\mathrm{CS,U}}(\phi) \equiv \frac{\mathcal{D}_{\mathrm{CS,U}}}{\mathcal{S}_{\mathrm{CS,U}}}$$

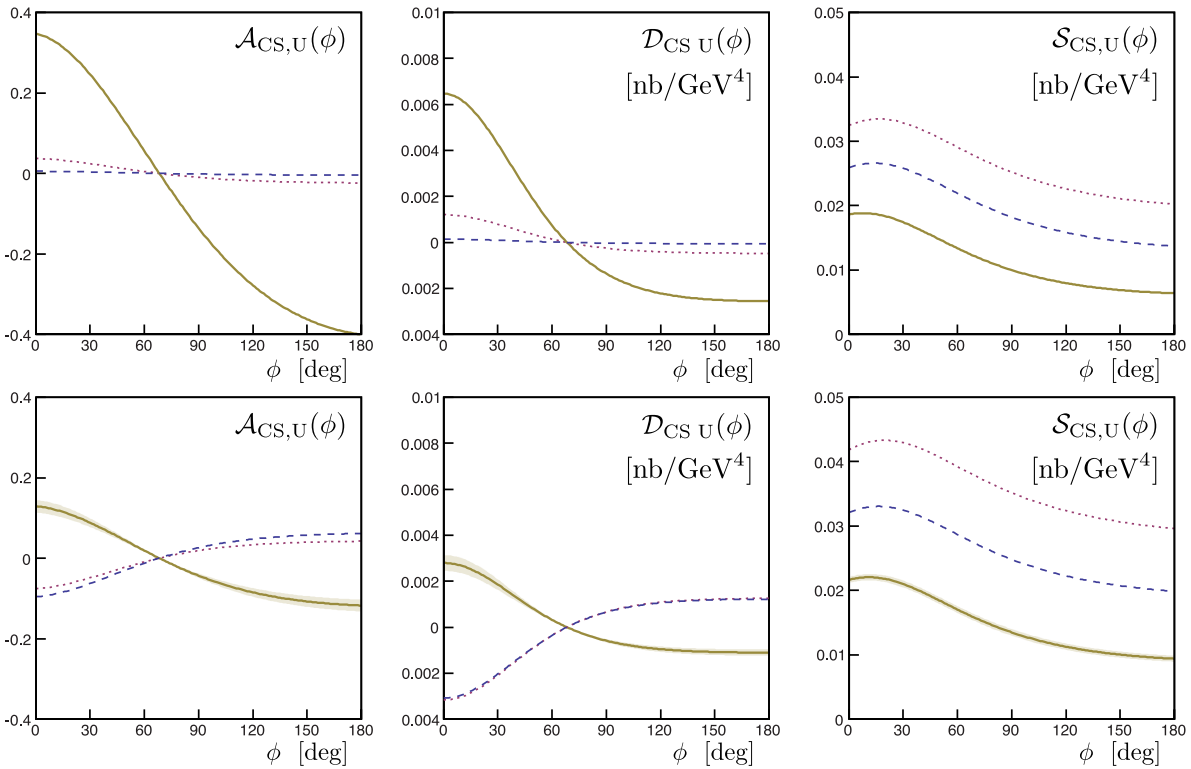

Figure: $\xi = 0.05, Q^2 = 4$ GeV^2, $t = -0.2$ GeV^2. On the first line- GK model, on the second line -factorized MSTW08 parametrization. In all plots, the LO result is shown as the dotted line, the full NLO result by the solid line and the NLO result without the gluonic contribution as the dashed line.

TCS and Bethe-Heitler contribution to exlusive lepton pair photoproduction.

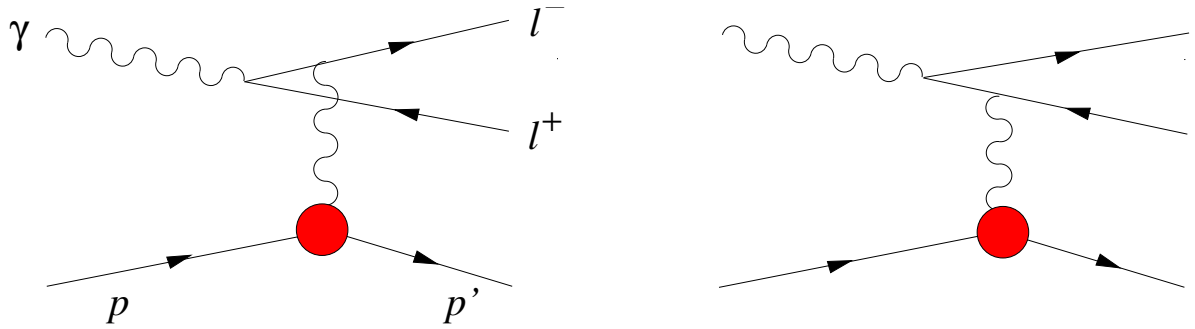

Figure: The Feynman diagrams for the Bethe-Heitler amplitude.

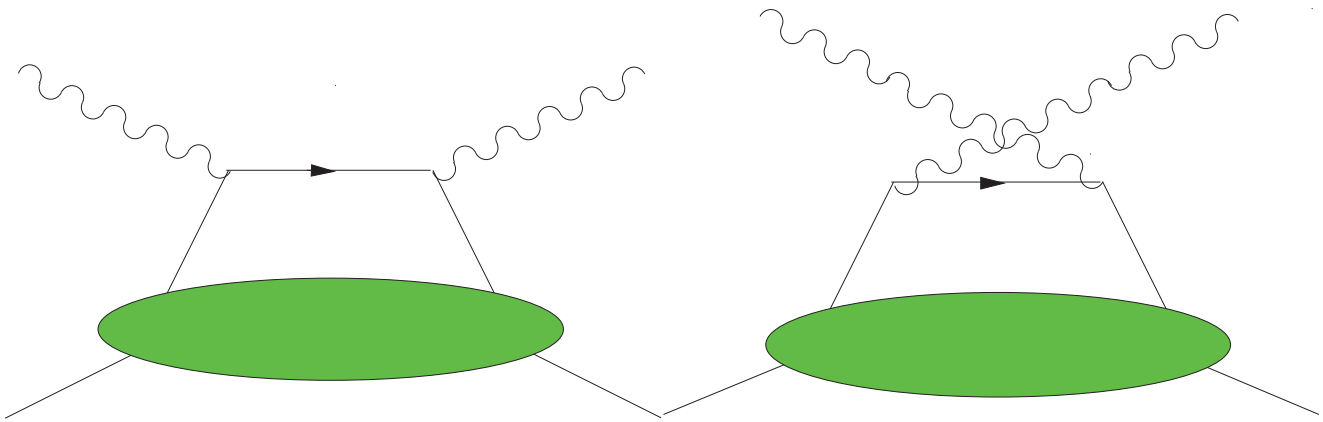

Figure: Handbag diagrams for the Compton process in the scaling limit.

TCS

Berger, Diehl, Pire, 2002

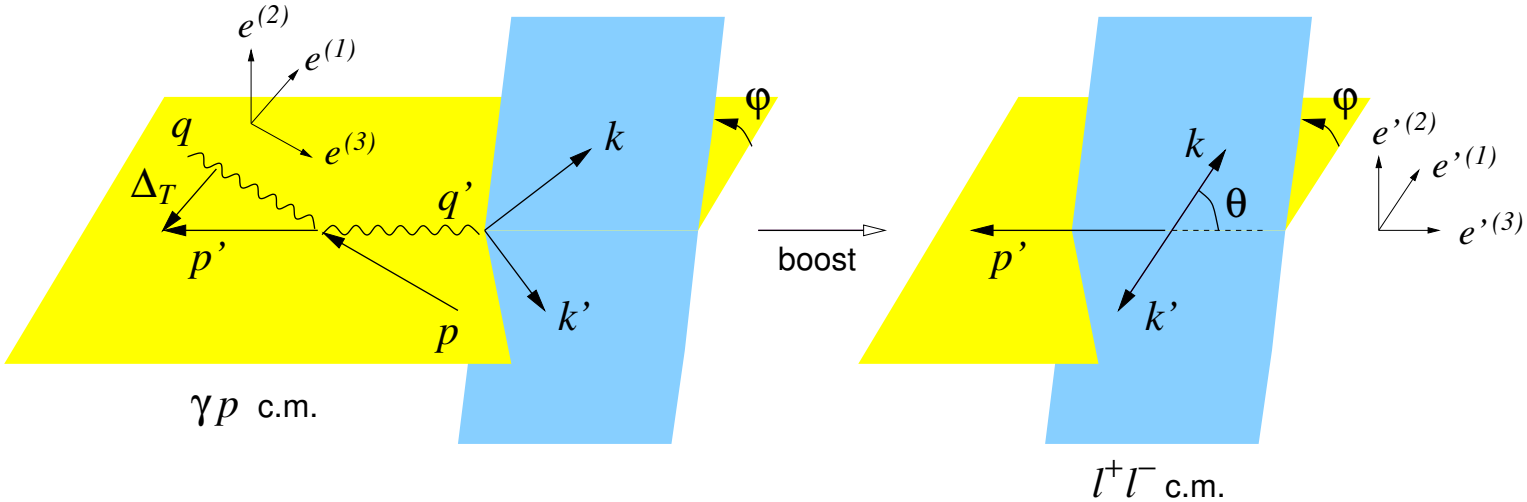

Figure: Kinematical variables and coordinate axes in the γp and $\ell^+\ell^-$ c.m. frames.

Interference

B-H dominant for not very high energies:

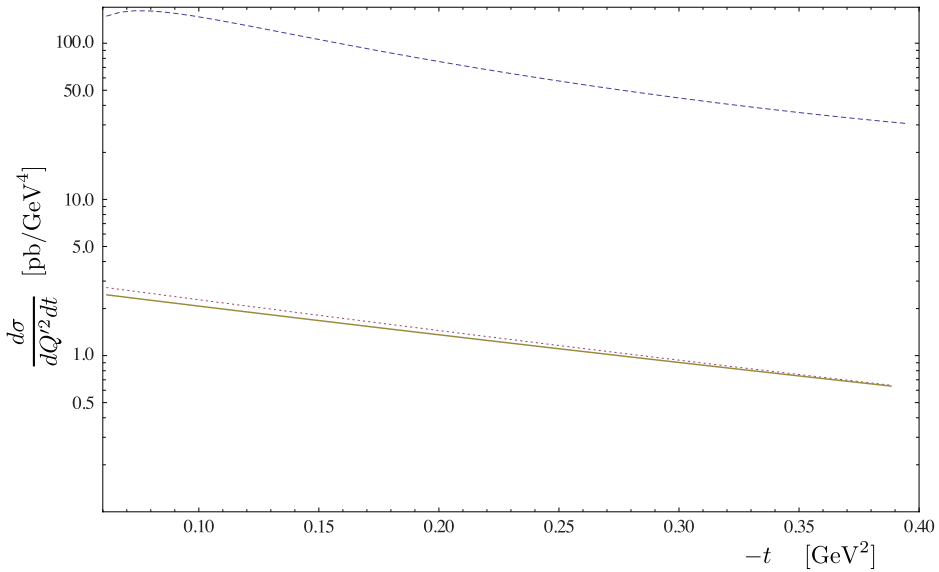

The interference part of the cross-section for $\gamma p \to \ell^+ \ell^- p$ with unpolarized protons and photons is given by:

$$\frac{d\sigma_{INT}}{dQ'^2\, dt\, d\cos\theta\, d\varphi} \sim \cos\varphi\ \mathrm{Re}\,\mathcal{H}(\xi, t)$$

Linear in GPD's, odd under exchange of the l^+ and l^- momenta $\Rightarrow$ angular distribution of lepton pairs is a good tool to study interference term.

JLAB 6 GeV data

Rafayel Paremuzyan PhD thesis

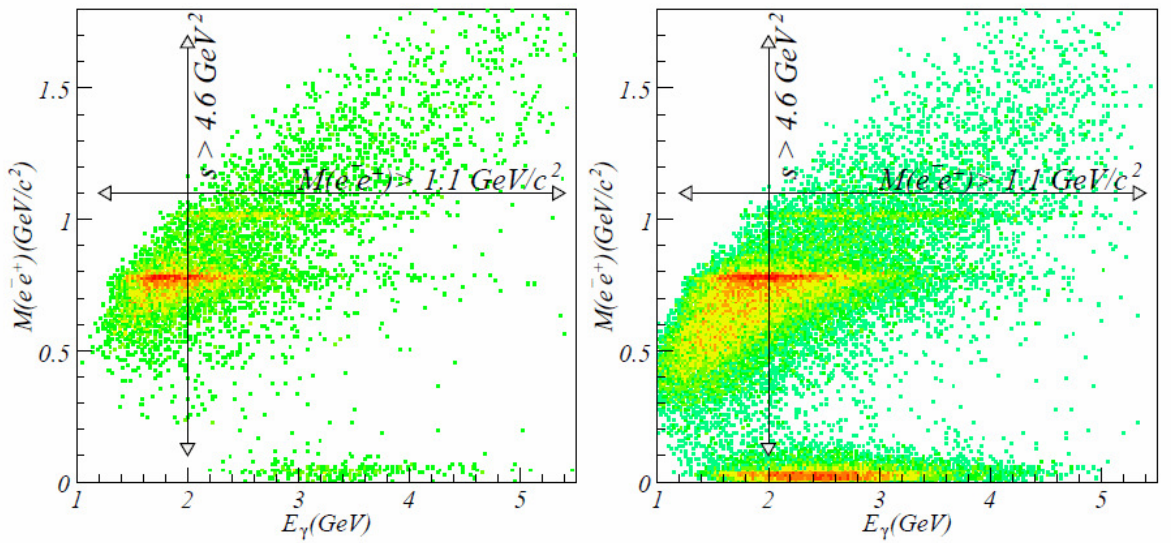

Figure: e^+e^- invariant mass distribution vs quasi-real photon energy. For TCS analysis $M(e^+e^-) > 1.1\,\mathrm{GeV}$ and $s_{\gamma p} > 4.6\,\mathrm{GeV}^2$ regions are chosen. Left graph represents e1-6 data set, right one is from e1f data set.

There is more data from g12 data set, soon to be analyzed. 12 GeV upgrade enables exploration of invariant masses up to $Q^2 = 9\,\mathrm{GeV}^2$ mass. Approved experiment in HALL B, planned experiment in HALL A.

Theory vs experiment

R.Paremuzyan and V.Guzey:

$$R = \frac{\int d\phi \ \cos\phi \ d\sigma}{\int \ d\phi \ d\sigma}$$

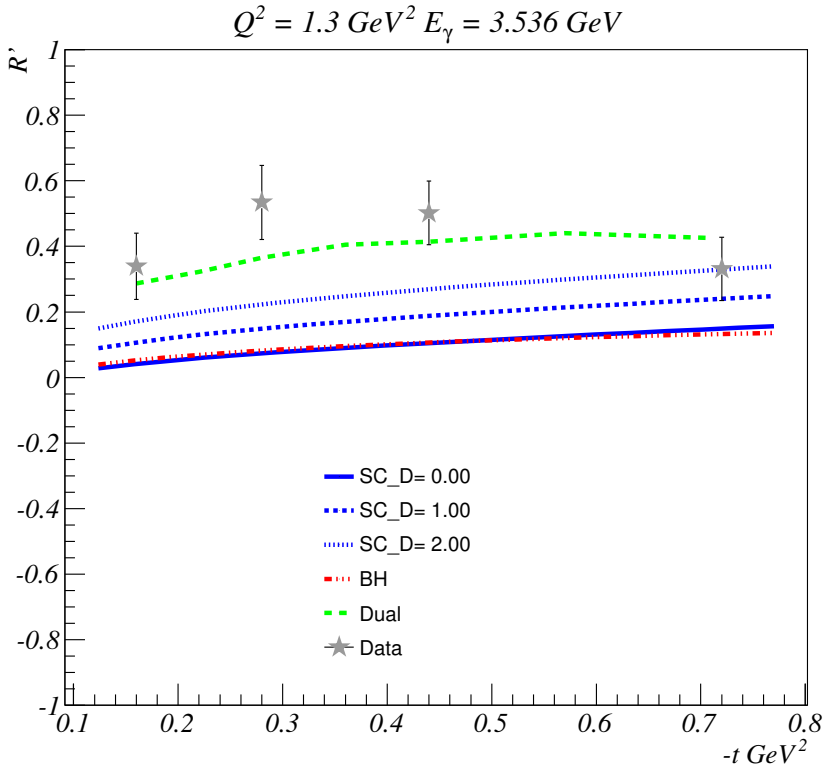

Figure: Thoeretical prediction of the ratio R for various GPDs models. Data points after combining both e1-6 and e1f data sets.

TCS

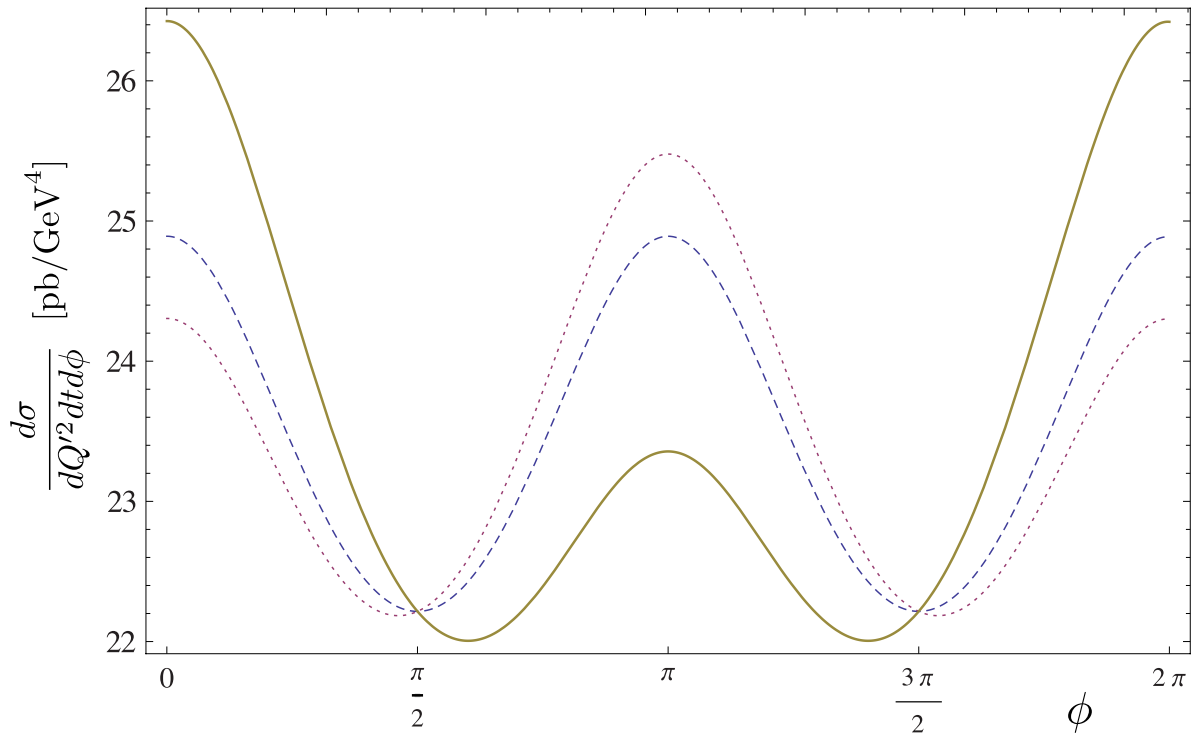

Figure: The ϕ dependence of the cross-section at $E_\gamma = 10$ GeV, $Q^2 = \mu^2 = 4$ GeV^2, and $t = -0.1$ GeV^2 integrated over $\theta \in (\pi/4, 3\pi/4)$: pure Bethe-Heitler contribution (dashed), Bethe-Heitler plus interference contribution at LO (dotted) and NLO (solid).

TCS

$$R(\eta) = \frac{2\int_0^{2\pi} d\varphi \, \cos\varphi \, \frac{dS}{dQ'^2 dt d\varphi}}{\int_0^{2\pi} d\varphi \, \frac{dS}{dQ'^2 dt d\varphi}} \,,$$

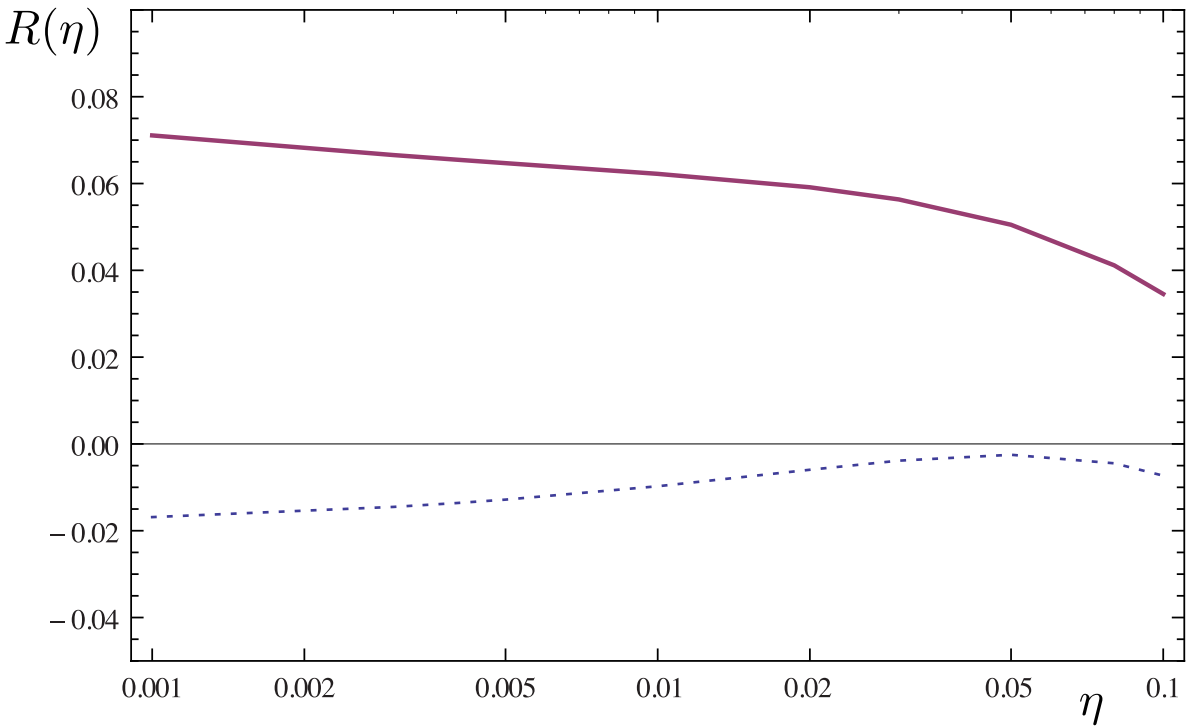

Figure: Ratio R defined as a function of η, for $Q^2 = \mu_F^2 = 4$ GeV^2 and $t = -0.1$ GeV^2. The dotted line represents LO contribution and the solid line represents NLO result.

TCS

The photon beam circular polarization asymmetry

$$A = \frac{\sigma^+ - \sigma^-}{\sigma^+ + \sigma^-} ,$$

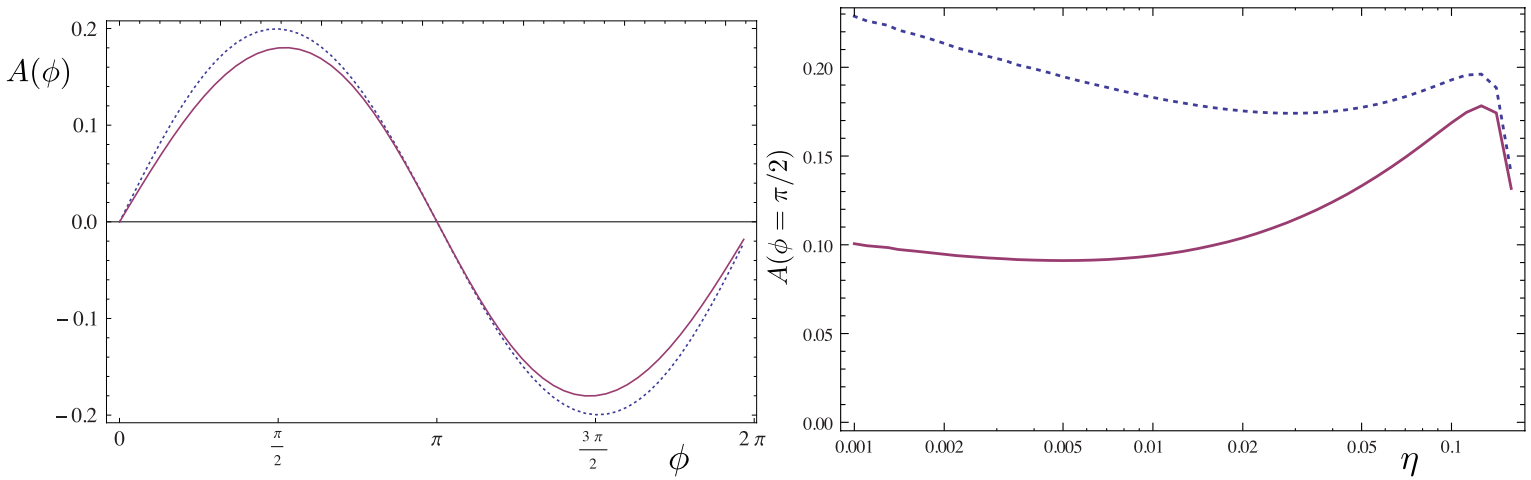

Figure: (Left) Photon beam circular polarization asymmetry as a function of ϕ, for $t = -0.1$ GeV^2, $Q^2 = \mu^2 = 4$ GeV^2, integrated over $\theta \in (\pi/4, 3\pi/4)$ and for $E_\gamma = 10$ GeV ($\eta \approx 0.11$). (Right) The η dependence of the photon beam circular polarization asymmetry for $Q^2 = \mu^2 = 4$ GeV^2, and $t = -0.2$ GeV^2 integrated over $\theta \in (\pi/4, 3\pi/4)$. The LO result is shown as the dotted line, the full NLO result by the solid line.

Summary

- inclusion of NLO corrections to the coefficient function is an important issue,
- difference of these corrections between the spacelike and timelike regimes is sizeable,
- importance of gluon contributions to the DVCS amplitude, even when the skewness variable η is in the so-called valence region. This effect is particularly big when one considers the real part of CFFs in the timelike case. This promotes the observables related to this quantity as sensitive probes of the three-dimensional gluon content of the nucleon.
- TCS already measured in JLAB 6 GeV, but much richer and more interesting kinematical region available after upgrade to 12 GeV,
- Better understanding of large terms (π^2, ??) is needed - factorization scheme? resummation ? ($\rightarrow$ Samuel Wallon talk)
- NLO corrections very important for small ξ's - EIC and LHeC.
- Compton scattering in ultraperipheral collisions at hadron colliders opens a new way to measure generalized parton distributions at small ξ's - experimentally challenging.

Ultraperipheral collisions

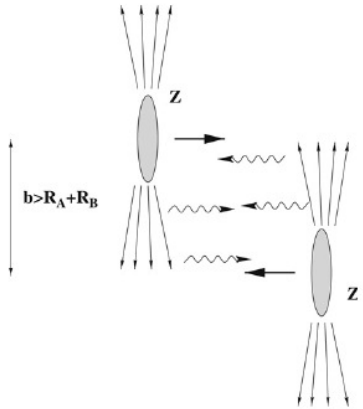

$$\sigma_{pp} = 2 \int \frac{dn(k)}{dk} \sigma_{\gamma p}(k) dk$$

$\sigma_{\gamma p}(k)$ is the cross section for the $\gamma p \to p l^+ l^-$ process and k is the γ's energy, and $\frac{dn(k)}{dk}$ is an equivalent photon flux.

For $\theta = [\pi/4, 3\pi/4]$, $\phi = [0, 2\pi]$, $t = [-0.05\,\mathrm{GeV}^2, -0.25\,\mathrm{GeV}^2]$, $Q'^2 = [4.5\,\mathrm{GeV}^2, 5.5\,\mathrm{GeV}^2]$, and photon energies $k = [20, 900]\,\mathrm{GeV}$ we get:

$$\sigma_{pp}^{BH} = 2.9\mathrm{pb}\ .$$

The Compton contribution gives:

$$\sigma_{pp}^{TCS} = 1.9\mathrm{pb}\ .$$

The interference cross section

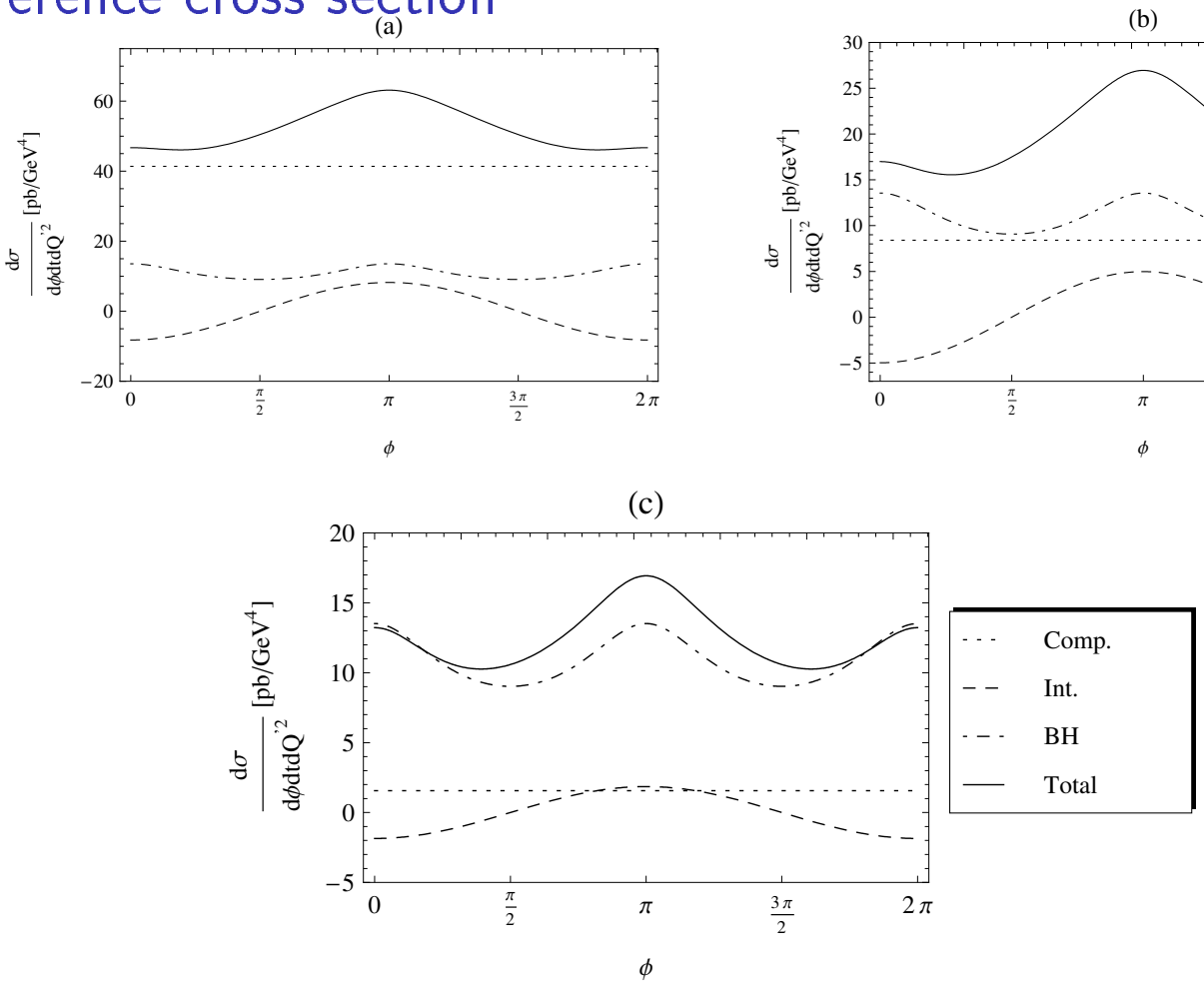

Figure: The differential cross sections (solid lines) for $t = -0.2\,\mathrm{GeV}^2$, $Q'^2 = 5\,\mathrm{GeV}^2$ and integrated over $\theta = [\pi/4, 3\pi/4]$, as a function of φ, for $s = 10^7\,\mathrm{GeV}^2$ (a), $s = 10^5\,\mathrm{GeV}^2$(b), $s = 10^3\,\mathrm{GeV}^2$ (c) with $\mu_F^2 = 5\,\mathrm{GeV}^2$. We also display the Compton (dotted), Bethe-Heitler (dash-dotted) and Interference (dashed) contributions.

Ultraperipheral collisions at RHIC

$$L \cdot k \frac{dn}{dk} (\mathrm{mb}^{-1}\mathrm{sec}^{-1})$$

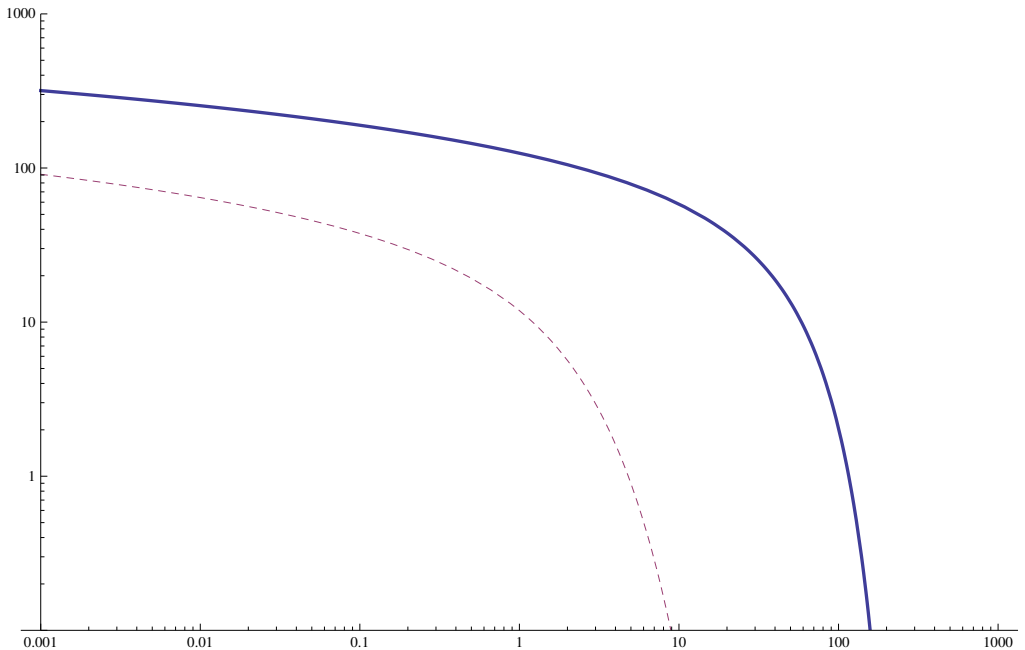

Figure: Effective luminosity of the photon flux from the Au-Au (dashed) and proton-proton (solid) collisions as a function of photon energy k(GeV).

RHIC

$\frac{d\sigma^{AuAu}}{dQ^2 dt d\phi}(\mu\text{b GeV}^{-4})$

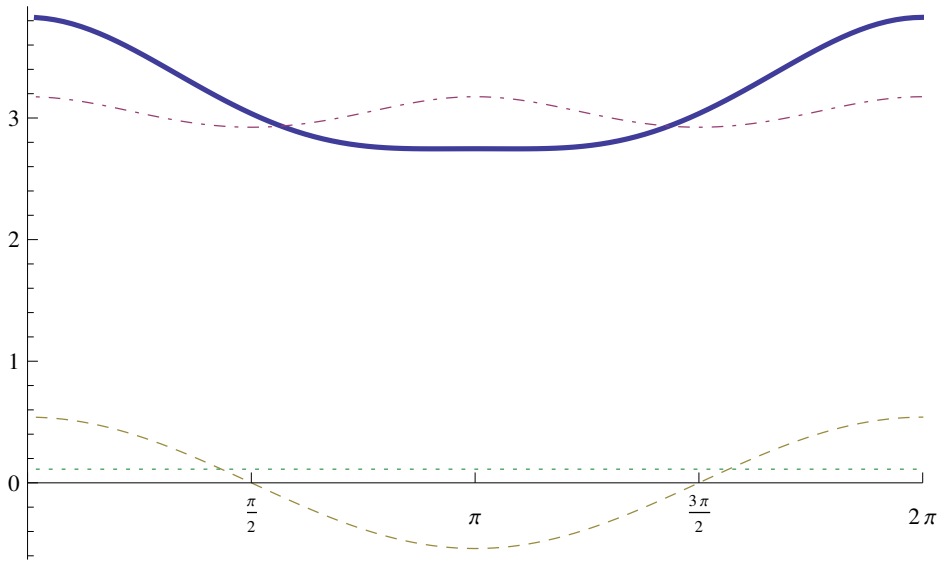

Figure: The differential cross sections (solid lines) for $t = -0.1\,\text{GeV}^2$, $Q'^2 = 5\,\text{GeV}^2$ and integrated over $\theta = [\pi/4, 3\pi/4]$, as a function of φ. We also display the Compton (dotted), Bethe-Heitler (dash-dotted) and Interference (dashed) contributions.

Total BH cross section (for $Q \in (2, 2.9)\,\text{GeV}$, $t \in (-0.2, -0.05)\,\text{GeV}^2$, $\theta = [\pi/4, 3\pi/4]$ and $\phi \in (0, 2\pi)$)

$$\sigma_{BH} = 41\mu\text{b} \qquad \text{Rate} = 0.04\text{Hz}$$

RHIC

$\frac{d\sigma^{pp}}{dQ^2 dt d\phi}(\text{pb GeV}^{-4})$

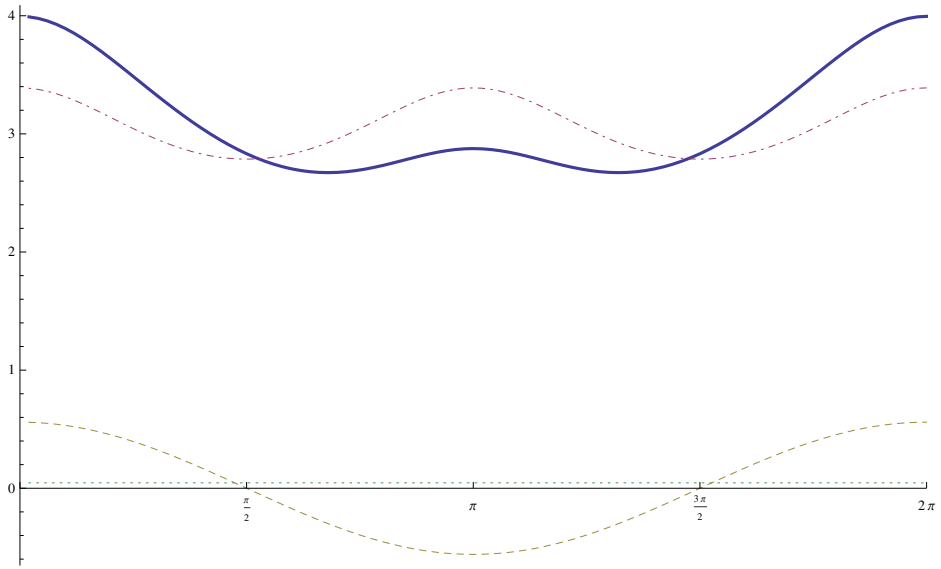

Figure: The differential cross sections (solid lines) for $t = -0.1\,\text{GeV}^2$, $Q'^2 = 5\,\text{GeV}^2$ and integrated over $\theta = [\pi/4, 3\pi/4]$, as a function of φ. We also display the Compton (dotted), Bethe-Heitler (dash-dotted) and Interference (dashed) contributions.

Total BH cross section (for $Q \in (2, 2.9)\,\text{GeV}$, $t \in (-0.2, -0.05)\,\text{GeV}^2$, $\theta = [\pi/4, 3\pi/4]$ and $\phi \in (0, 2\pi)$)

$$\sigma_{BH} = 9\text{pb} \qquad \text{Rate} = 5/\text{day}$$